Evaluation of the increased load bearing capacity of steel beams strengthened with pre-stressed FRP laminates

S. Bennati, D. Colonna, P.S. Valvo
Università di Pisa, Dipartimento di Ingegneria Civile e Industriale, Largo Lucio Lazzarino, 56122 Pisa, Italy
s.bennati@ing.unipi.it, p.valvo@ing.unipi.it

ABSTRACT. We analyse the problem of a simply supported steel beam subjected to uniformly distributed load, strengthened with a pre-stressed fibre-reinforced polymer (FRP) laminate. We assume that the laminate is first put into tension, then bonded to the beam bottom surface, and finally fixed at both its ends by suitable connections. The beam and laminate are modelled according to classical beam theory. The adhesive is modelled as a cohesive interface with a piecewise linear constitutive law defined over three intervals (elastic response, softening response, debonding). The model is described by a set of differential equations with suitable boundary conditions. An analytical solution to the problem is determined, including explicit expressions for the internal forces and interfacial stresses. As an application, we consider the standard IPE series for the steel beam and the Sika® CarboDur® system for the adhesive and laminate. For each considered cross section, we first carry out a preliminary design of the unstrengthened steel beam. Then, we imagine to apply the FRP strengthening and calculate the loads corresponding to the elastic limit states in the steel beam, adhesive, and laminate. Lastly, we take into account the ultimate limit state corresponding to the plasticisation of the mid-span steel cross section and evaluate the increased load bearing capacity of the strengthened beam.

KEYWORDS. Steel beam; FRP strengthening; Adhesive; Beam theory; Cohesive-zone model; Analytical solution; Pre-stressing; Ultimate limit state; Load bearing capacity.

Citation: Bennati, S., Colonna, D., Valvo, P.S., Evaluation of the increased load bearing capacity of steel beams strengthened with pre-stressed FRP laminates, Frattura ed Integrità Strutturale, 38 (2016) 377-391.

Received: 15.08.2016
Accepted: 08.09.2016
Published: 01.10.2016

INTRODUCTION

Fibre-reinforced polymers (FRP) are increasingly used in civil engineering for the strengthening of existing constructions. In such applications, the existing structural elements (made of traditional materials such as, for instance, masonry, wood, concrete, steel, etc.) are strengthened by adhesively bonding FRP laminates onto their external surfaces. The type of fibre, shape, thickness, and other characteristics of the laminate vary according to the

element to be strengthened and the desired level of structural performance [1]. For the strengthening of steel structures, carbon fibre reinforced polymers (CFRP) are preferred because of their superior mechanical properties [2, 3]. Furthermore, CFRP laminates can be pre-stressed, which enables more effective use of the composite material, contribution of the strengthening in carrying out the dead load, closure of cracks in concrete [4, 5], and increased fatigue life in steel [6].

The existing structure and FRP laminate behave as a composite structure with a key role played by the adhesive layer, which transfers the stresses between the bonded elements. As a matter of fact, debonding of the FRP laminate due to high interfacial stresses is a relevant failure mode for this type of interventions. Therefore, a wide number of theoretical and experimental studies have been conducted to achieve reliable and accurate evaluation of such interfacial stresses. Smith and Teng [7] presented a review of the theoretical models for predicting the interfacial stresses and also developed a solution for strengthened beams in bending. Al-Emrani and Kliger [8] determined the interfacial shear stresses in beams strengthened with pre-stressed laminates subjected to mid-span concentrated loads. Benachour et al. [9] extended the previous solutions to distributed loads and multidirectional laminates used as strengthening. All the aforementioned models consider the adhesive layer as an elastic interface to obtain simple closed-form solutions. A more realistic modelling of the adhesive can be achieved by introducing a non-linear (or piecewise linear) cohesive law for the interface [10–12].

Bennati et al. [13] used a cohesive-zone model to determine the overall non-linear response of an FRP-strengthened beam in pure bending. In a preliminary version of the present paper [14], such model has been extended to account for the pre-stressing of the laminate. The beam is considered simply supported and subjected to uniformly distributed load. According to the assumed application technology, the laminate is first put into tension, then bonded to the beam bottom surface, and finally fixed at both its ends by suitable connections. The beam and laminate are modelled according to classical beam theory. The adhesive is modelled as a cohesive interface with a piecewise linear constitutive law defined over three intervals (elastic response, softening response, debonding). The model is described by a set of differential equations with suitable boundary conditions. Here, we determine an analytical solution to the stated problem, including explicit expressions for the internal forces and interfacial stresses. As an application, we consider the standard IPE series [15] for the steel beam and the Sika® CarboDur® system [16] for the FRP strengthening. The latter consists of an epoxy resin adhesive (Sikadur-30®) and pultruded carbon fibre-reinforced polymer laminates (CarboDur® S). For each considered steel cross section, we first carry out a preliminary design to determine the length and permanent load of the "existing" unstrengthened beam. Then, we imagine to apply the FRP strengthening and calculate the loads corresponding to the elastic limit states in the steel beam, adhesive, and laminate. Lastly, we take into account the ultimate limit state corresponding to the plasticisation of the mid-span steel cross section and evaluate the increased load bearing capacity of the strengthened beam [17, 18]. Calculations are carried out according to the Eurocodes [19–21] and Italian regulations on FRP strengthening [22, 23].

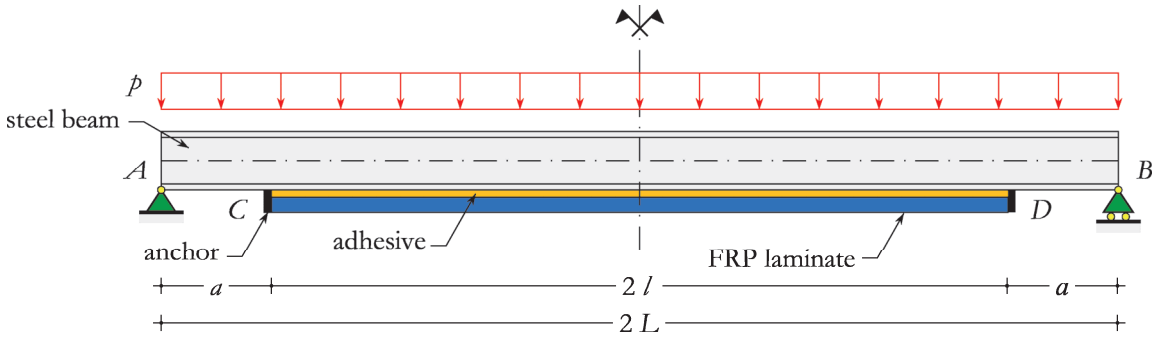

Figure 1: FRP-strengthened steel beam subjected to uniformly distributed load.

MECHANICAL MODEL

Let us consider an I-section steel beam AB of length $2L$, simply supported at its ends and subjected to a uniformly distributed load per unit length, p (Fig. 1). As better specified in the following, the load p will actually be a combination of the beam self-weight, g_1, a permanent load due to non-structural elements, g_2, and an imposed load, q. The beam is strengthened by an FRP laminate of length $2l$ adhesively bonded to its bottom surface. As concerns the application technique, we assume that the laminate is first pre-stressed by a suitable axial force, P, then adhesively

bonded to the beam, and finally fixed at both its end sections, C and D. We denote with $a = L - l$ the distance of the anchor points from the end sections of the beam.
We denote with b_b and h_b respectively the width and height of the steel cross section and with h_f the thickness of the flange (Fig. 2). Furthermore, we indicate with A_b, I_b, W_b, and Z_b respectively the area, moment of inertia, elastic modulus, and plastic modulus of the cross section of the beam. Besides, we denote with b_f and t_f respectively the width and thickness of the laminate and with t_a the thickness of the adhesive layer. Lastly, we indicate with $A_f = b_f t_f$ the area of the cross section of the laminate.

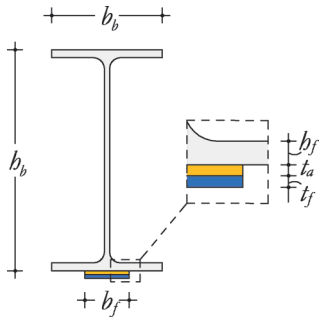

Figure 2: Cross section of the strengthened beam.

Thanks to symmetry, the model can be limited to the left-hand half system (Fig. 3). The generic cross section of the beam is identified by a curvilinear abscissa, s, measured from the anchor point of the laminate, C. Similarly, the generic cross section of the laminate is identified by a curvilinear abscissa, s^*, also measured from point C. We denote with $w_b(s)$ the axial displacements of points at the beam bottom surface and with $w_f(s^*)$ the axial displacements of the laminate cross sections.

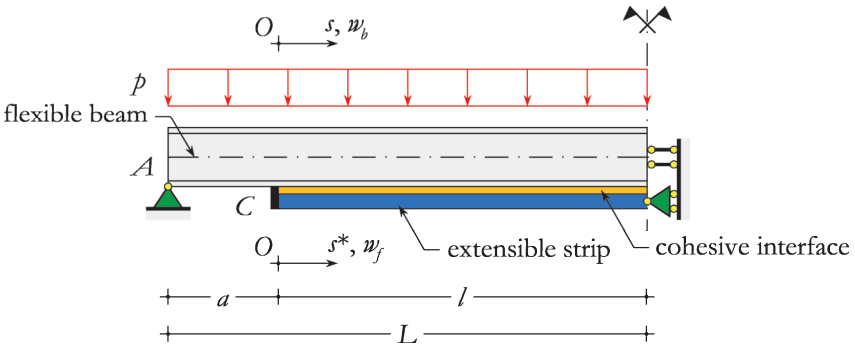

Figure 3: Mechanical model of the strengthened beam.

In the proposed mechanical model, the steel beam is considered as a flexible beam, while the FRP laminate is modelled as an extensible strip. An elastic-perfectly plastic behaviour is assumed for steel with Young's modulus E_s and design yield stress f_{yd} (Fig. 4a). The behaviour of FRP is assumed elastic-brittle with Young's modulus E_f and design tensile strength f_{fd} (Fig. 4b). The adhesive layer is represented by a zero-thickness cohesive interface, which transfers shear stresses, τ, and no normal stresses. The interfacial stresses depend on the relative displacements, $\Delta w = w_f - w_b$, between the laminate and the bottom surface of the beam. The interface behaviour is assumed linearly elastic for shear stresses up to a limit value, τ_0; then, a linear softening stage, corresponding to progressive damage, follows; lastly, debonding occurs. For $\Delta w \geq 0$, the cohesive interface law is given by the following piecewise linear relationship (Fig. 4c):

$$\tau(\Delta w) = \begin{cases} k\,\Delta w, & 0 \leq \Delta w \leq \Delta w_0 \quad \text{(elastic response)} \\ k_s(\Delta w_u - \Delta w), & \Delta w_0 < \Delta w \leq \Delta w_u \quad \text{(softening response)} \\ 0, & \Delta w_u < \Delta w \quad \text{(debonding)} \end{cases} \tag{1}$$

where k and k_s are the elastic constants for the elastic and softening responses, respectively; Δw_0 and Δw_u are the relative displacements at the elastic limit and start of debonding, respectively. The elastic constant for the elastic response can be taken as $k = G_a / t_a$, where G_a is the shear modulus of the adhesive.

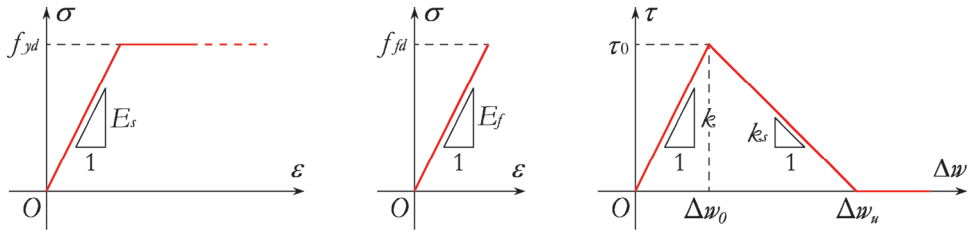

Figure 4: Constitutive laws: (a) steel, (b) FRP, (c) adhesive.

STRUCTURAL RESPONSE

To determine the structural response of the FRP-strengthened beam, it is necessary to distinguish between different stages of behaviour. In what follows, stage 0 refers to the unstrengthened beam, subjected to its self-weight and permanent loads. In stage 1, the laminate is pre-stressed and fixed to the beam. At this point, there is yet no composite action between the beam and laminate, which however are both stressed and deformed because of the dead load and pre-stressing. In stage 2, the beam and laminate behave as an elastic composite structure under the imposed loads. This stage ends when one of the composing elements – beam, laminate, or adhesive – reaches its elastic limit. In stage 3, non-linear response is expected due to plasticity of the steel beam and/or softening of the adhesive layer. However – as the numerical examples will show – the steel beam turns out to be always the weakest element. Therefore, the load bearing capacity of the system is governed by the plasticisation of the steel beam.

Stage 0 – Unstrengthened beam

The unstrengthened beam is subjected to its self-weight, g_1, and permanent loads, g_2, both assumed here as uniformly distributed. Such loads will cause both stress and deformation, however within the linearly elastic behaviour regime. At this stage, the axial force, shear force, and bending moment in the beam respectively are

$$N_{b,G}(s)=0,\quad V_{b,G}(s)=(g_1+g_2)(l-s),\quad M_{b,G}(s)=\frac{1}{2}(g_1+g_2)(a+l)(2l+a-s) \tag{2}$$

with $-a \le s \le l$. When evaluating ultimate limit states, loads in Eq. (2) should be suitably factored [19, 21].
In real applications, cambering of the beam is often introduced to compensate for the deflection due to dead loads. For simplicity, here we do not consider any cambering and assume the deformed configuration of the unstrengthened beam as the reference configuration for strains and displacements.

Stage 1 – Pre-stressing and fixing of the laminate

During the pre-stressing stage, the laminate is put into tension by an axial force, $N_{f,P} = P$, applied through the anchor points on the beam bottom surface. Simultaneously, the beam is compressed by the same axial force, which produces also bending because of the eccentricity of the load application point with respect to the beam centreline. The internal forces produced by pre-stressing in the strengthened part of the beam ($0 \le s \le l$) are

$$N_{b,P}(s)=-N_{f,P}=-P,\quad V_{b,P}(s)=0,\quad M_{b,P}(s)=-\frac{1}{2}Ph_b \tag{3}$$

The internal forces given by Eqs. (3) are to be added to those given by Eqs. (2) to obtain the total internal forces in the beam at the end of the pre-stressing stage. All loads should be suitable factored when evaluating ultimate limit states.

Due to pre-stressing, points belonging to the beam bottom surface will move towards the mid-span cross section; conversely, points on the laminate will move towards the anchor point *C*. From the classic assumption of beam theory, that plane sections remain plane, and the constitutive laws for the beam and laminate, we determine the following (positive) displacement for a point *S* on the beam bottom surface at the abscissa *s*:

$$w_{b,P}(s)=P\left(\frac{1}{E_sA_b}+\frac{h_b^2}{4E_sI_b}\right)(l-s) \tag{4}$$

and the following (negative) displacement for a point *S** of the laminate at the abscissa *s**:

$$w_{f,P}(s^*)=-\frac{P}{E_fA_f}(l-s^*) \tag{5}$$

On curing of the adhesive, the beam and laminate behave as a composite structure. To determine the interfacial stresses through Eq. (1), the relative displacements at the interface should be evaluated with respect to the deformed configuration at the end of the pre-stressing stage. To this aim, we consider that points *S* and *S**, initially not aligned, be placed on the same cross section at the end of the pre-stressing operation (Fig. 5).

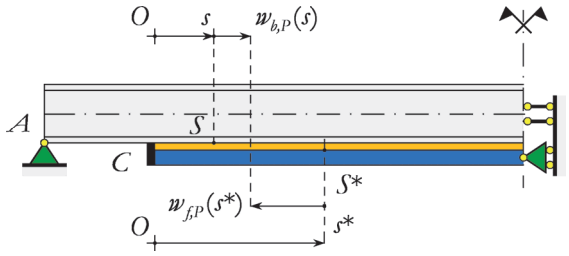

Figure 5: Displacements of beam and laminate at the end of the pre-stressing stage.

Alignment of points *S* and *S** after pre-stressing requires that

$$s+w_{b,P}(s)=s^*+w_{f,P}(s^*) \tag{6}$$

By substituting Eqs. (4) and (5) into (6), we determine the following relationship between *s* and *s**:

$$s^*(s)=\frac{\left(\frac{1}{E_sA_b}+\frac{h_b^2}{4E_sI_b}+\frac{1}{E_fA_f}\right)l-\left(\frac{1}{E_sA_b}+\frac{h_b^2}{4E_sI_b}-\frac{1}{P}\right)s}{\frac{1}{E_fA_f}+\frac{1}{P}} \tag{7}$$

Stage 2 – Application of imposed loads – Linear response

When imposed loads are applied to the strengthened beam, the relative displacement at the interface (with respect to stage 1) turns out to be

$$\Delta w(s)=w_{f,Q}(s^*)-w_{f,P}(s^*)-w_{b,Q}(s)+w_{b,P}(s) \tag{8}$$

where $w_{b,Q}(s)$ and $w_{f,Q}(s^*)$ respectively are the axial displacements of the beam bottom surface and laminate produced by the imposed load, *q*. In Eq. (8), the abscissa *s** should be calculated through Eq. (7). For $\Delta w \le \Delta w_0$, the interface behaves elastically, so that Eq. (1) yields the interface shear stress

$$\tau(s) = k\left[w_{f,Q}(s^*) - w_{f,P}(s^*) - w_{b,Q}(s) + w_{b,P}(s) \right] \tag{9}$$

Fig. 6 shows a free-body diagram of an elementary segment of the strengthened beam included between the cross sections at s and $s + ds$. From static equilibrium, the following equations are deduced:

$$\begin{aligned} &\frac{dN_{b,Q}(s)}{ds} = -b_f \tau(s) \\ &\frac{dV_{b,Q}(s)}{ds} = -q \\ &\frac{dM_{b,Q}(s)}{ds} = V_{b,Q}(s) - \frac{1}{2} b_f h_b \tau(s) \\ &N_{f,Q}(s) = -N_{b,Q}(s) \end{aligned} \tag{10}$$

where $N_{b,Q}$, $V_{b,Q}$, and $M_{b,Q}$ respectively are the axial force, shear force, and bending moment in the beam; $N_{f,Q}$ is the axial force in the laminate due to the imposed load. By solving the differential problem defined by Eqs. (9) and (10) – as explained in the Appendix – the following expressions are obtained for the interfacial shear stress,

$$\tau(s) \cong \xi q \left[l - s - l \exp(-\lambda s) \right] \tag{11}$$

and internal forces in the beam,

$$\begin{aligned} &N_{b,Q}(s) = \xi q b_f \left\{ s\left(\frac{1}{2} s - l \right) + \frac{l}{\lambda} \left[1 - \exp(-\lambda s) \right] \right\} \\ &V_{b,Q}(s) = q(l - s) \\ &M_{b,Q}(s) = \frac{1}{2} q(a + s)(2l + a - s) + \frac{1}{2} \xi q b_f h_b \left\{ s\left(\frac{1}{2} s - l \right) + \frac{l}{\lambda} \left[1 - \exp(-\lambda s) \right] \right\} \end{aligned} \tag{12}$$

where ξ and λ are constant parameters defined by Eq. (A10) in the Appendix.

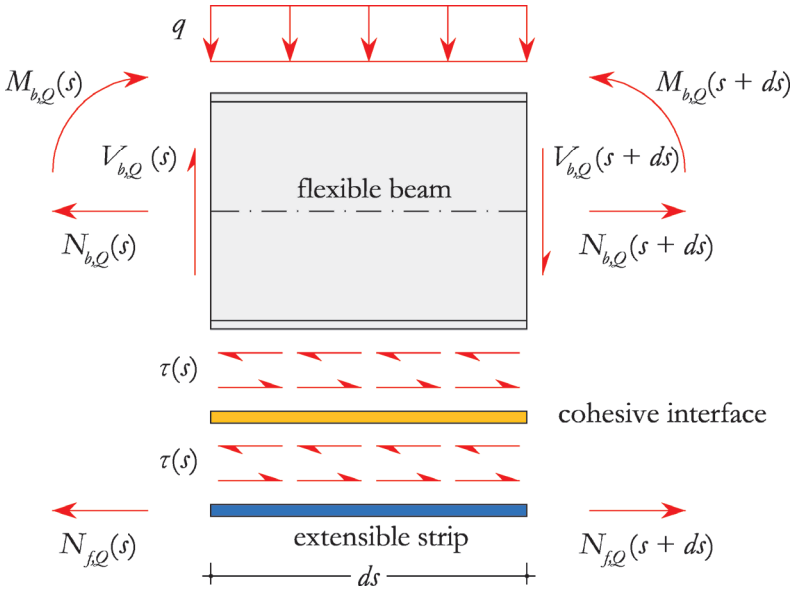

Figure 6: Free-body diagram of an elementary beam segment.

Stage 3 – Application of imposed loads – Non-linear response and failure of the system

In stage 3, non-linear response is expected due to either plasticity of the steel beam or softening of the adhesive. However, as the numerical examples below will demonstrate, for current material properties and geometry, the steel beam turns out to be the weakest element of the system, while the adhesive behaves elastically up to very high values of the imposed load. A detailed description of the structural response in stage 3 would require considering the progressive plasticisation of the beam at the mid-span and neighbouring cross sections. At the same time, large deformations and displacements are expected to occur, bringing further non-linearity into the problem. For the sake of simplicity, here we do not explicitly analyse the above sketched non-linear response and limit ourselves to consider the ultimate limit state corresponding to the complete plasticisation of the mid-span cross section of the beam.

APPLICATION

For illustration purposes, we apply the model to standard IPE steel beams [15]. For each cross section of the series from IPE 120 to IPE 600, we first carry out a preliminary design to determine the span and permanent load of the "existing" unstrengthened beam. Then, we imagine to apply the Sika® CarboDur® FRP strengthening system [16] and calculate the loads corresponding to the elastic limit states in the beam, adhesive, and laminate. Lastly, we take into account the ultimate limit state corresponding to the plasticisation of the mid-span steel cross section and evaluate the increased load bearing capacity of the strengthened beam.

Material properties and geometry of structural elements

The material properties, factored according to the Eurocodes [20, 21] and Italian regulations on FRP strengthening [22, 23], are the following:

- steel (grade S235): Young's modulus, E_s = 210 GPa; characteristic yield stress, f_{yk} = 235 MPa; partial factor for material, γ_s = 1.05; design yield stress, $f_{yd} = f_{yk} / \gamma_s$ = 223.81 MPa;
- adhesive (Sikadur®-30): shear modulus, G_a = 4.923 GPa; characteristic strength, τ_k = 15 MPa; environmental conversion factor, η_a = 0.85; partial factor for material, γ_a = 1.2; design strength, $\tau_0 = \eta_a \tau_k / \gamma_a$ = 10.63 MPa;
- laminate (CarboDur® S): longitudinal Young's modulus, E_f = 165 GPa; characteristic tensile strength, f_{fk} = 3100 MPa; partial factor for material, γ_f = 1.1; design tensile strength, $f_{fd} = \eta_a f_{fk} / \gamma_f$ = 2395.45 MPa.

Concerning the geometry of structural elements, the geometric properties of the steel cross sections are listed in Tab. 1. The thickness of the adhesive layer is assumed t_a = 1 mm. The laminates have width b_f = 60 mm and thickness t_f = 1.3 (type S613) or 2.6 mm (type S626), depending on the steel cross section. The distance between the beam supports and laminate anchor points is a = 500 mm for all cross sections.

Cross section	Width b_b (mm)	Height h_b (mm)	Flange thickness h_f (mm)	Area A_b (mm^2)	Moment of inertia I_b (mm^4)	Elastic section modulus W_b (mm^3)	Plastic section modulus Z_b (mm^3)
IPE 120	64	120	6.3	1321	3178000	52960	60730
IPE 140	73	140	6.9	1643	5412000	77320	88340
IPE 160	82	160	7.4	2009	8693000	108700	123900
IPE 180	91	180	8.0	2395	13170000	146300	166400
IPE 200	100	200	8.5	2848	19430000	194300	220600
IPE 220	110	220	9.2	3337	27720000	252000	285400
IPE 240	120	240	9.8	3912	38920000	324300	366600
IPE 270	135	270	10.2	4595	57900000	428900	484000
IPE 300	150	300	10.7	5381	83560000	557100	628400
IPE 330	160	330	11.5	6261	117700000	713100	804300
IPE 360	170	360	12.7	7273	162700000	903600	1019000
IPE 400	180	400	13.5	8446	231300000	1156000	1307000
IPE 450	190	450	14.6	9882	337400000	1500000	1702000
IPE 500	200	500	16.0	11550	482000000	1928000	2194000
IPE 550	210	550	17.2	13440	671200000	2441000	2787000
IPE 600	220	600	19.0	15600	920800000	3069000	3512000

Table 1: Geometric properties of steel cross sections.

Pre-sizing of steel beams

The span of the "existing" beam, $2L$, and permanent load due to non-structural elements, g_2, are fixed by assuming that, under the action of dead loads, the maximum stress in the mid-span cross section of the beam is less than 33% of the yield stress and the mid-span deflection is less than 1/800 of the span:

$$\begin{cases} \frac{1}{8}(g_1+g_2)(2L)^2 \le 0.33 f_{yd} W_b \\ \frac{5}{384}\frac{g_1+g_2}{E_s I_b}(2L)^4 \le \frac{1}{800}(2L) \end{cases} \tag{13}$$

By taking the equal sign in inequalities (13), the maximum theoretical values of $2L$ and g_2 are first determined. Then, by rounding down such values to the nearest integer multiples of 500 mm and 0.50 kN/m, respectively, the final values assumed in subsequent calculations are determined (see Tab. 2).

Cross section	Length $2L$ (mm)	Permanent load g_2 (kN/m)
IPE 120	2000	7.0
IPE 140	2000	7.5
IPE 160	2500	8.0
IPE 180	3000	8.5
IPE 200	3000	9.5
IPE 220	3500	10.0
IPE 240	4000	11.0
IPE 270	4500	11.5
IPE 300	5000	12.0
IPE 330	5500	12.5
IPE 360	6000	13.5
IPE 400	6500	14.0
IPE 450	7500	14.0
IPE 500	8500	14.5
IPE 550	9000	15.0
IPE 600	10000	16.0

Table 2: Pre-sizing of steel beams.

Pre-stressing of FRP laminates

The pre-stressing tensile axial force in the FRP laminates is assumed to correspond to 50% of the design tensile strength:

$$P = 0.50\frac{f_{fk}}{\gamma_f}A_f \tag{14}$$

Depending on the steel cross section, one or two laminates CarboDur® type S613 or S626 are used, as illustrated in Tab. 3. The Table also shows the normal stresses at the upper and lower surfaces of the mid-span cross section of the beam, σ_1^- and σ_1^+, respectively, produced by the dead loads and pre-stressing. By recalling Eqs. (2) and (3), such stresses can be computed as follows:

$$\sigma_1^{\pm} = \frac{N_{b,G}(l) + N_{b,P}(l)}{A_b} \pm \frac{M_{b,G}(l) + M_{b,P}(l)}{W_b} = -\frac{P}{A_b} \pm \frac{1}{2}\frac{(g_1 + g_2)L^2 - Ph_b}{W_b} \tag{15}$$

It can be verified that all the computed values are in magnitude less than the design yield stress, f_{yd}.

Cross section	No. and type of laminates	Width b_f (mm)	Thickness t_f (mm)	Area A_f (mm²)	Pre-stressing force P (kN)	Stress at upper surface σ_1^- (MPa)	Stress at lower surface σ_1^+ (MPa)
IPE 120	1 S613	60	1.3	78	109.9	-25.7	-140.7
IPE 140	1 S613	60	1.3	78	109.9	-16.7	-117.1
IPE 160	1 S613	60	1.3	78	109.9	-32.4	-77.0
IPE 180	1 S613	60	1.3	78	109.9	-45.1	-46.7
IPE 200	1 S626	60	2.6	156	219.8	-20.3	-134.0
IPE 220	1 S626	60	2.6	156	219.8	-32.2	-99.5
IPE 240	1 S626	60	2.6	156	219.8	-44.5	-67.8
IPE 270	1 S626	60	2.6	156	219.8	-48.6	-47.1
IPE 300	1 S626	60	2.6	156	219.8	-51.3	-30.4
IPE 330	1 S626	60	2.6	156	219.8	-53.1	-17.1
IPE 360	2 S626	120	2.6	312	439.6	-42.9	-78.0
IPE 400	2 S626	120	2.6	312	439.6	-42.9	-61.2
IPE 450	2 S626	120	2.6	312	439.6	-47.7	-41.2
IPE 500	2 S626	120	2.6	312	439.6	-53.1	-23.0
IPE 550	2 S626	120	2.6	312	439.6	-49.7	-15.7
IPE 600	2 S626	120	2.6	312	439.6	-55.3	-1.1

Table 3: Pre-stressing of FRP laminates.

Elastic limit state of the system

Now, we turn to evaluate the imposed load for which the strengthened beam abandons the range of linearly elastic behaviour. This load will be the minimum between the loads corresponding to the elastic limit states in the beam, adhesive, and laminate. We start from the elastic limit state of the adhesive, which occurs when the maximum shear stress in the interface reaches the design strength, τ_0. The abscissa, $\bar{s}$, where the shear stress is maximum is first determined by differentiating Eq. (11) and setting the derivative to zero:

$$\frac{d\tau}{ds} \cong -\xi q + \xi q \lambda l \exp(-\lambda \bar{s}) = 0 \quad \Rightarrow \quad \bar{s} = \frac{1}{\lambda}\ln(\lambda l) \tag{16}$$

Hence, the maximum shear stress value turns out to be

$$\tau_{\max} = \tau(\bar{s}) = q\xi\left\{l - \frac{1}{\lambda}\left[1 + \ln(\lambda l)\right]\right\} \tag{17}$$

By putting $\tau_{\max} = \tau_0$, the corresponding imposed load is obtained,

$$q_a = \frac{1}{\gamma_Q}\frac{1}{\xi}\frac{\tau_0}{l - \frac{1}{\lambda}\left[1 + \ln(\lambda l)\right]} \tag{18}$$

where γ_Q = 1.5 is the partial factor for variable actions [19, 21].

Moving on to consider the elastic limit state of the laminate, we observe that the maximum axial force, $N_{f\max}$, occurs at the mid-span cross section of the beam. By recalling Eqs. (3), (10), and (12), we obtain

$$N_{f\max} = \gamma_P N_{f,P} + \gamma_Q N_{f,Q}(l) = \gamma_P P - \gamma_Q q \xi b_f \left\{ -\frac{l^2}{2} + \frac{l}{\lambda}\left[1-\exp(-\lambda l)\right] \right\} \tag{19}$$

where $\gamma_P = 1.0$ is the partial factor for pre-stressing actions [19, 21]. By putting $N_{f\max} = f_{fd} A_f$, the corresponding imposed load is obtained,

$$q_f = \frac{1}{\gamma_Q}\frac{1}{\xi b_f}\frac{f_{fd}A_f - \gamma_P P}{\frac{l^2}{2} - \frac{l}{\lambda}\left[1-\exp(-\lambda l)\right]} \tag{20}$$

Lastly, we consider the elastic limit state of the beam. To this aim, the normal stresses at the upper and lower surfaces of the mid-span cross section of the beam, σ_2^- and σ_2^+, respectively, are computed. By recalling Eqs. (2), (3), and (12), we find

$$\begin{aligned}\sigma_2^{\pm} &= \frac{\gamma_G N_{b,G}(l) + \gamma_P N_{b,P}(l) + \gamma_Q N_{b,Q}(l)}{A_b} \pm \frac{\gamma_G M_{b,G}(l) + \gamma_P M_{b,P}(l) + \gamma_Q M_{b,Q}(l)}{W_b} = \\ &= \pm\frac{1}{2}\frac{\gamma_{G1}g_1 + \gamma_{G2}g_2}{W_b}L^2 - \left(\frac{1}{A_b} \pm \frac{h_b}{2}\frac{1}{W_b}\right)\left\{\gamma_P P + \gamma_Q q \xi b_f l\left[\frac{l}{2} - \frac{1}{\lambda} + \frac{1}{\lambda}\exp(-\lambda l)\right]\right\} \pm \frac{1}{2}\gamma_Q q \frac{L^2}{W_b}\end{aligned} \tag{21}$$

where γ_G (equal to $\gamma_{G1} = 1.3$ for the self-weight, g_1, and $\gamma_{G1} = 1.5$ for the other dead loads, g_2) represents the partial factor for permanent actions. Hence, by putting $\sigma_2^- = -f_{yd}$ and $\sigma_2^+ = f_{yd}$, respectively, and taking the minimum between the two resulting values of the imposed load, we obtain the imposed load corresponding to the elastic limit state of the beam,

$$q_b = \frac{1}{\gamma_Q}\min\left\{ \frac{f_{yd} - \frac{1}{2}\frac{\gamma_{G1}g_1 + \gamma_{G2}g_2}{W_b}L^2 + \gamma_P P\left(\frac{1}{A_b} + \frac{h_b}{2}\frac{1}{W_b}\right)}{\frac{1}{2}\frac{L^2}{W_b} - \xi b_f l\left(\frac{1}{A_b} + \frac{h_b}{2}\frac{1}{W_b}\right)\left[\frac{l}{2} - \frac{1}{\lambda} + \frac{1}{\lambda}\exp(-\lambda l)\right]}; \right. \\ \left. \frac{f_{yd} - \frac{1}{2}\frac{\gamma_{G1}g_1 + \gamma_{G2}g_2}{W_b}L^2 - \gamma_P P\left(\frac{1}{A_b} - \frac{h_b}{2}\frac{1}{W_b}\right)}{\frac{1}{2}\frac{L^2}{W_b} + \xi b_f l\left(\frac{1}{A_b} - \frac{h_b}{2}\frac{1}{W_b}\right)\left[\frac{l}{2} - \frac{1}{\lambda} + \frac{1}{\lambda}\exp(-\lambda l)\right]} \right\} \tag{22}$$

Tab. 4 summarises the results obtained by applying Eqs. (18), (20), and (22). The weakest element turns out to be always the steel beam, whose yielding stress determines the load corresponding to the elastic limit state of the system.

Evaluation of increased bearing capacity

To evaluate the increase in the load bearing capacity given by the strengthening system, we first calculate the load bearing capacity of the unstrengthened steel beam. The imposed load, q_u, corresponding to the complete plasticisation of the mid-span cross section of the beam is calculated as follows:

$$\frac{1}{2}(\gamma_{G1}g_1 + \gamma_{G2}g_2 + \gamma_Q q)L^2 = M_p \quad \Rightarrow \quad q_u = q = \frac{1}{\gamma_Q}\left(\frac{2}{L^2}M_p - \gamma_{G1}g_1 - \gamma_{G2}g_2\right) \tag{23}$$

where $M_p = f_{yd} Z_b$ is the plastic moment of the steel cross section.

Cross section	Limit load for adhesive q_a (kN/m)	Limit load for laminate q_f (kN/m)	Limit load for beam q_b (kN/m)
IPE 120	878.8	405.8	11.7
IPE 140	1257.1	580.3	18.9
IPE 160	1136.3	353.8	15.1
IPE 180	1122.5	263.8	12.7
IPE 200	785.1	366.2	20.4
IPE 220	795.9	298.6	17.8
IPE 240	838.0	262.9	15.8
IPE 270	935.5	252.3	16.0
IPE 300	1050.2	248.4	16.5
IPE 330	1183.2	249.2	17.3
IPE 360	1390.2	263.9	19.8
IPE 400	1597.5	276.1	21.8
IPE 450	1731.6	253.7	20.4
IPE 500	1909.7	242.8	19.4
IPE 550	2249.1	268.3	22.9
IPE 600	2495.4	264.8	22.2

Table 4: Imposed loads at elastic limit states.

Cross section	Load bearing capacity of unstrengthened beam q_u (kN/m)	Load bearing capacity of strengthened beam q_s (kN/m)	Increase in load bearing capacity Δq (kN/m)	Percent increase Δq / q_u (%)
IPE 120	11.0	15.9	4.8	43.7
IPE 140	18.8	25.6	6.8	36.4
IPE 160	15.5	21.7	6.1	39.6
IPE 180	13.4	19.0	5.6	42.0
IPE 200	19.6	27.4	7.8	39.8
IPE 220	17.6	24.8	7.2	40.8
IPE 240	16.1	23.1	7.0	43.8
IPE 270	16.7	24.1	7.4	43.9
IPE 300	17.6	25.2	7.5	42.7
IPE 330	18.8	25.7	6.9	36.4
IPE 360	19.8	28.7	8.9	45.0
IPE 400	22.4	32.5	10.2	45.5
IPE 450	21.5	31.7	10.2	47.5
IPE 500	21.0	29.8	8.8	42.0
IPE 550	25.2	33.8	8.7	34.4
IPE 600	24.9	32.5	7.6	30.7

Table 5: Load bearing capacity of the system.

Moving on to the strengthened beam, the results of the previous section suggest that the ultimate limit state of the system corresponds to plasticisation of the steel beam and not to debonding of the adhesive or rupture of the laminate. In the strengthened beam, the mid-span cross section is subjected to both axial force and bending moment. According to the

Eurocodes [20], Eq. (23) can still be used, provided that M_p is replaced by M_{pN}, which takes into account a possible reduction of the plastic moment due to the axial force:

$$M_{pN} = \begin{cases} \min\left\{1, \quad \dfrac{1-n_b}{1-0.5a_b}\right\} M_p, & \text{for } n_b \le a_b \\ \left[1-\left(\dfrac{n_b-a_b}{1-a_b}\right)^2\right] M_p, & \text{for } n_b > a_b \end{cases} \tag{24}$$

where, in our notation,

$$n_b = \frac{\gamma_G N_{b,G}(l) + \gamma_P N_{b,P}(l) + \gamma_Q N_{b,Q}(l)}{f_{yd} A_b} \quad \text{and} \quad a_b = \min\left\{1 - 2\frac{b_b b_f}{A_b}, \quad 0.5\right\} \tag{25}$$

By substituting Eqs. (2), (3), and (12) into (23)–(25), and solving for q, the load bearing capacity of the strengthened beam, q_s, is determined. Tab. 5 summarises the results obtained for the analysed cases, showing the increase in the load bearing capacity of the system, $\Delta q = q_s - q_u$. The percent increase ranges between 30% and 50%.

Conclusions

We have presented the mechanical model of a simply supported steel beam subjected to uniformly distributed load, strengthened with a pre-stressed FRP laminate. An analytical solution has been determined for the differential problem that describes the structural response of the strengthened beam. The model has been applied to study IPE steel beams strengthened by using the Sika® CarboDur® FRP strengthening system. Analysis of the elastic limit states in the steel beam, adhesive, and laminate has shown that the steel beam is always the weakest element of the system. The softening response of the adhesive is not reached in practice being preceded by the plasticisation of steel. For the sake of simplicity, however, we have not analysed the non-linear structural response resulting from the progressive plasticisation of the beam at the mid-span and neighbouring cross sections. This behaviour could indeed be the subject of future studies, which should also take into account the expected large deformations and displacements, as well as the possible lateral torsional buckling. Here, the complete plasticisation of the mid-span cross section of the steel beam has been assumed as the ultimate limit state of the system. Correspondingly, the increased load bearing capacity of the strengthened beam has been evaluated.

References

[1] Bank, L.C., Composites for Construction, John Wiley & Sons, New Jersey (2006).
[2] Zhao, X.-L., Zhang, L., State-of-the-art review on FRP strengthened steel structures, Eng. Struct., 29 (2007) 1808–1823.
[3] Gholami, M., Sam, A.R.M., Yatim, J.M., Tahir, M.M., A review on steel/CFRP strengthening systems focusing environmental performance, Constr. Build. Mater., 47 (2013) 301–310.
[4] Aslam, M., Shafigh, P., Jumaat, M.Z., Shah, S.N.R., Strengthening of RC beams using prestressed fiber reinforced polymers – A review, Constr. Build. Materi., 82 (2015) 235–256.
[5] Haghani, R., Al-Emrani, M., Kliger, R., A new method for strengtheng concrete structures using prestressed FRP laminates, in: Saha, S., Zhang, Y., Yazdani, S., Singh, A. (eds.), Proc. 8th International Structural Engineering and Construction Conference – ISEC 2015: Implementing Innovative Ideas in Structural Engineering and Project Management, Sydney, Australia (2015).
[6] Ghafoori, E., Motavalli, M., Zhao, X.-L., Nussbaumer, A., Fontana, M., Fatigue design criteria for strengthening metallic beams with bonded CFRP plates, Eng. Struct., 101 (2015) 542–557.
[7] Smith, S.T., Teng, J.G., Interfacial stresses in plated beams. Engineering Structures, 23(2001) 857–871.

[8] Al-Emrani, M., Klieger, R., Analysis of interfacial shear stresses in beams strengthened with bonded prestressed laminates, Compos. Part B – Eng., 37 (2006) 265–272.
[9] Benachour, A., Benyoucef, S., Tounsi, A., Adda Bedia, E.A., Interfacial stress analysis of steel beams reinforced with bonded prestressed FRP plate, Eng. Struct., 30 (2008) 3305–3315.
[10] De Lorenzis, L., Zavarise, G., Cohesive zone modeling of interfacial stresses in plated beams, Int. J. Solids Struct., 46 (2009) 4181–4191.
[11] Cornetti, P., Carpinteri, A., Modelling the FRP-concrete delamination by means of an exponential softening law, Eng. Struct., 33 (2011) 1988–2001.
[12] Cornetti, P., Corrado, M., Lorenzis, L.D., Carpinteri, A., An analytical cohesive crack modeling approach to the edge debonding failure of FRP-plated beams, Int. J. Solids Struct., 53 (2015) 92-106.
[13] Bennati, S., Dardano, N., Valvo, P.S., A mechanical model for FRP-strengthened beams in bending, Frattura ed Integrità Strutturale, 22 (2012) 39–55.
[14] Bennati, S., Colonna, D., Valvo, P.S., A cohesive-zone model for steel beams strengthened with pre-stressed laminates, Procedia Structural Integrity, 2 (2016) 2682–2689.
[15] EN 19:1957, IPE beams: I-beams with parallel flange facings.
[16] Sika® AG, www.sika.com.
[17] Linghoff, D., Al-Emrani, M., Kliger, R., Performance of steel beams strengthened with CFRP laminate – Part 1: Laboratory tests, Compos. Part B – Eng., 41 (2010) 509–515.
[18] Linghoff, D., Al-Emrani, M., Performance of steel beams strengthened with CFRP laminate – Part 2: FE analyses, Compos, Part B – Eng., 41 (2010) 516–522.
[19] EN 1990:2002+A1:2005, Eurocode: Basis of structural design.
[20] EN 1993-1-1:2005, Eurocode 3: Design of steel structures – Part 1–1: General rules and rules for buildings.
[21] Ministero delle Infrastrutture e dei Trasporti, Decreto 31 luglio 2012, Approvazione delle Appendici nazionali recanti i parametri tecnici per l'applicazione degli Eurocodici, Rome, Italy (2013).
[22] CNR-DT 200 R1/2013, Istruzioni per la Progettazione, l'Esecuzione ed il Controllo di Interventi di Consolidamento Statico mediante l'utilizzo di Compositi Fibrorinforzati, Rome, Italy (2005).
[23] CNR-DT 202/2005, Studi Preliminari finalizzati alla redazione di Istruzioni per Interventi di Consolidamento Statico di Strutture Metalliche mediante l'utilizzo di Compositi Fibrorinforzati, Rome, Italy (2005).

ACKNOWLEDGEMENTS

Financial support from the ERA-NET Plus Infravation 2014 Call within the project SUREBridge (www.surebridge.eu) through subcontract by partner company AICE Consulting Srl (www.aiceconsulting.it) is gratefully acknowledged.

APPENDIX

Formulation of the differential problem

The axial strains at the bottom surface of the beam and in the laminate due to the applied load, q, can be defined respectively as

$$\varepsilon_{b,Q}(s)=\frac{dw_{b,Q}(s)}{ds} \quad \text{and} \quad \varepsilon_{f,Q}(s^*)=\frac{dw_{f,Q}(s^*)}{ds^*} \tag{A1}$$

Besides, from Navier's equation and the constitutive laws for the beam and laminate, we have

$$\varepsilon_{b,Q}=\frac{N_{b,Q}}{E_s A_b}+\frac{M_{b,Q}}{E_s I_b}\frac{h_b}{2} \quad \text{and} \quad \varepsilon_{f,Q}=\frac{N_{f,Q}}{E_f A_f} \tag{A2}$$

In order to formulate the differential problem through a single equation, we start by differentiating Eq. (9) with respect to s:

$$\frac{d\tau}{ds}=k\left(\frac{dw_{f,Q}}{ds*}\frac{ds*}{ds}-\frac{dw_{f,P}}{ds*}\frac{ds*}{ds}-\frac{dw_{b,Q}}{ds}+\frac{dw_{b,P}}{ds}\right) \tag{A3}$$

Then, we differentiate also Eq. (7) with respect to s and obtain the following expression, whose numerical values turn out to be approximately equal to 1 for current geometric and material properties:

$$\frac{ds*}{ds}=\frac{\frac{1}{P}-\frac{1}{E_sA_b}-\frac{h_b^2}{4E_sI_b}}{\frac{1}{P}+\frac{1}{E_fA_f}}\cong 1 \tag{A4}$$

By substituting Eqs. (4), (5), and (A1) into (A3), and considering (A4), we obtain

$$\frac{d\tau}{ds}\cong -k\left[\varepsilon_{b,Q}-\varepsilon_{f,Q}+P\left(\frac{1}{E_sA_b}+\frac{h_b^2}{4E_sI_b}+\frac{1}{E_fA_f}\right)\right] \tag{A5}$$

By further differentiating Eq. (A5) and recalling (A2), we have

$$\frac{d^2\tau}{ds^2}=-k\left(\frac{d\varepsilon_{b,Q}}{ds}-\frac{d\varepsilon_{f,Q}}{ds}\right)=-k\left(\frac{1}{E_sA_b}\frac{dN_{b,Q}}{ds}+\frac{h_b}{2E_sI_b}\frac{dM_{b,Q}}{ds}-\frac{1}{E_fA_f}\frac{dN_{f,Q}}{ds}\right) \tag{A6}$$

Lastly, by substituting Eqs. (10) into (A6), after simplification, we obtain the following differential equation for the interfacial shear stress:

$$\frac{d^2\tau}{ds^2}-kb_f\left(\frac{1}{E_sA_b}+\frac{h_b^2}{4E_sI_b}+\frac{1}{E_fA_f}\right)\tau(s)=-k\frac{h_b}{2E_sI_b}V_{b,Q}(s) \tag{A7}$$

where the shear force is

$$V_{b,Q}(s)=q(l-s). \tag{A8}$$

Solution of the differential problem

The differential problem stated in the previous section can be solved analytically. In fact, the general solution to Eq. (A7) for the interfacial shear stress is

$$\tau(s)=C_1\exp(\lambda s)+C_2\exp(-\lambda s)+\xi q(l-s) \tag{A9}$$

where C_1 and C_2 are integration constants and the constant parameters

$$\lambda=\sqrt{kb_f\left(\frac{1}{E_sA_b}+\frac{h_b^2}{4E_sI_b}+\frac{1}{E_fA_f}\right)}\quad\text{and}\quad \xi=\frac{k}{\lambda^2}\frac{h_b}{2E_sI_b}=\frac{h_b}{2b_f}\frac{1}{\frac{I_b}{A_b}+\left(\frac{h_b}{2}\right)^2+\frac{E_sI_b}{E_fA_f}} \tag{A10}$$

are also introduced. By imposing the boundary conditions,

$$\begin{cases}\tau(0)=0\\ \tau(l)=0\end{cases} \tag{A11}$$

we obtain

$$C_1 = -\frac{\xi q l}{1-\exp(2\lambda l)} \cong 0 \quad \text{and} \quad C_2 = -\frac{\xi q l}{1-\exp(-2\lambda l)} \cong -\xi q l \tag{A12}$$

where the approximations are justified by the values of the exponential functions in practical problems. Lastly, we obtain the following final expression for the interfacial shear stress:

$$\tau(s) \cong \xi q(l-s) - \xi q l \exp(-\lambda s) \tag{A13}$$

which is equivalent to Eq. (11) in the main text above. By substituting Eqs. (A8) and (A13) into (10) and integrating, we obtain

$$\begin{aligned} N_{b,Q}(s) &= -\frac{1}{2}\xi q b_f (2ls - s^2) - \xi q b_f \frac{l}{\lambda}\exp(-\lambda s) + C_3 \\ M_{b,Q}(s) &= \frac{1}{2}q(1-\frac{h_b}{2}\xi b_f)(2ls - s^2) - \frac{h_b}{2}\xi q b_f \frac{l}{\lambda}\exp(-\lambda s) + C_4 \end{aligned} \tag{A14}$$

where C_3 and C_4 are integration constants. These are determined by imposing the continuity of the axial force and bending moment at the cross section of the anchor point:

$$\begin{cases} N_{b,Q}(0) = 0 \\ M_{b,Q}(0) = \frac{1}{2}qa(2l+a) \end{cases} \tag{A15}$$

Hence,

$$C_3 = \xi q b_f \frac{l}{\lambda} \quad \text{and} \quad C_4 = \frac{1}{2}qa(2l+a) + \xi q b_f \frac{l}{\lambda}\frac{h_b}{2} \tag{A16}$$

The final expressions for the internal forces in the beam turn out to be

$$\begin{aligned} N_{b,Q}(s) &= \xi q b_f (\frac{l}{\lambda} - ls + \frac{1}{2}s^2) - \xi q b_f \frac{l}{\lambda}\exp(-\lambda s) \\ M_{b,Q}(s) &= \frac{1}{2}q(a+s)(2l+a-s) + \frac{1}{2}\xi q b_f h_b (\frac{l}{\lambda} - ls + \frac{1}{2}s^2) - \frac{1}{2}\xi q b_f h_b \frac{l}{\lambda}\exp(-\lambda s) \end{aligned} \tag{A17}$$

It can be easily verified that Eqs. (A8) and (A17) are equivalent to Eqs. (12) in the main text above.